Available online at www.sciencedirect.com
SCIENCE DIRECT®
Journal of Solid State Chemistry 178 (2005) 419–428
JOURNAL OF SOLID STATE CHEMISTRY
www.elsevier.com/locate/jssc

The standard and anomalous crystal-field spectra of Eu^{3+}

X.Y. Chen*, G.K. Liu

Chemistry Division, Argonne National Laboratory, Argonne, IL 60439-4803, USA

Received 4 May 2004; received in revised form 14 September 2004; accepted 16 September 2004
Available online 11 November 2004

Abstract

The crystal-field (CF) spectra of Eu^{3+} in various inorganic crystalline phases are summarized based on previous investigations. A majority of experimental results can be well interpreted using a standard CF model. However, there are cases in which the spectroscopic properties and fluorescence dynamics of Eu^{3+} cannot be interpreted within the framework of the standard model. A particularly interesting system is Eu^{3+} doped into microcrystals of a charge-unbalanced host such as BaFCl. For Eu^{3+}:BaFCl, one Eu^{3+} site (Site I) exhibits normal CF splitting and its energy levels and fluorescence intensity are similar to most other normal systems ever reported. A standard CF fitting has been performed for Site I. However, Eu^{3+} at a distorted site (Site II) is of anomalous fluorescence dynamics and CF splitting which are significantly different from those of Site I. In the metastable state of $^5D_0$, Eu^{3+} ions at Site II also exhibit unusual temperature-dependent lifetime.

Keywords: Crystal-field spectra; Eu^{3+}; Charge-transfer states; Energy levels; Wybourne–Downer mechanism

1. Introduction

The characteristics of the $4f^6$ energy-level structure and electronic transition intensity of Eu^{3+} have been extensively investigated in various crystals for several decades. In general, the crystal field (CF) is relatively weak in comparison with electrostatic and spin–orbit coupling because the partially filled $4f$ shell is shielded by the filled $5s$ and $5p$ orbitals. A majority of experimental results can be well interpreted using a standard spectroscopic model that allows diagonalization of the combined free-ion (FI) and CF energy matrices [1–3]. Occasionally, there are special cases in which the spectroscopic properties of an ion in $4f^6$ configuration cannot be interpreted within the framework of the standard model of CF interactions and fluorescence dynamics [4–13]. Unlike other rare-earth (RE) ions, the charge-transfer states (CTS) of Eu^{3+} in solids are much lower and lie near the $4f^6$ energy levels. The CTS are believed to be closely related to the anomalous CF spectra. As a result, charge-transfer (CT)-induced f-electron delocalization (or covalency) in solids may significantly influence the energy-level structure of Eu^{3+}, whereas the violation of the closure approximation assumed in Judd–Ofelt theory [14,15] may change the $4f$–$4f$ transition intensity pattern. In this paper, we first summarize the characteristics of standard and anomalous CF spectra of Eu^{3+} ions doping in inorganic crystal hosts. We then focus on new results from Eu^{3+} at two sites of BaFCl microcrystals, and discuss the anomalous spectroscopic properties which cannot be interpreted by the standard CF model.

2. Experimental

The microcrystals of 0.1 at% Eu:BaFCl were grown by solid-state reaction in the atmosphere of He. A stoichiometric mixture of BaF_2, $BaCl_2$, and EuF_3 were ground, placed in an Al_2O_3 crucible then heated at 300 °C (1 h) to drive out the moisture and then at 800 °C

*Corresponding author. Fax: +1 630 252 4225.
E-mail addresses: xchen70@anl.gov (X.Y. Chen), gkliu@anl.gov (G.K. Liu).

0022-4596/$ - see front matter © 2004 Elsevier Inc. All rights reserved.
doi:10.1016/j.jssc.2004.09.002

for one more hour. The TEM image of the as-prepared particles indicates an average particle size of approximately 1–2 μm. The energy dispersive X-ray spectrum and powder X-ray diffraction confirms the tetragonal crystalline phase of BaFCl.

For the site-selective fluorescence spectra, a pulsed dye laser with a tunable range from 510 to 580 nm, or an ultraviolet (UV) pulsed laser at 266 or 355 nm, was used to pump the samples. The dye laser wavelength was tuned to match the excitation transition $^7F_0 \rightarrow {}^5D_1$ of the Eu^{3+} ions at various sites. The fluorescence was dispersed by a monochrometer (SPEX 1704) at a spectral resolution of approximately 0.008 nm and detected with a cooled RCA C31034 photomultiplier. The signals were recorded using a gated boxcar (Stanford Research Systems, model SR250). The sample was mounted in a cryostat with temperature variable from 2 to 300 K. The fluorescence decay measurements were performed using a digital storage oscilloscope (Tektronix TDS 680C).

3. A summary of CF spectra of Eu^{3+}

3.1. Standard CF spectra of Eu^{3+}

Eu^{3+} ions are usually employed as a sensitive probe to investigate the coordination and local environment around the cations substituted in the crystalline lattice based on the fact that the $^5D_0$ and $^7F_0$ levels are not subjected to CF splitting while the splittings of the emission (or absorption) transitions involving the $^{2S+1}L_J$ multiplets with $J>0$ are symmetry-dependent [3,16]. In most cases, the CF splitting can be well interpreted by parameterization of a one-electron CF and FI model. The commonly used effective operator Hamiltonian is

$$H = H_{\mathrm{FI}} + H_{\mathrm{CF}}, \tag{1}$$

where the FI Hamiltonian can be expressed as follows:

$$\begin{aligned} H_{\mathrm{FI}} = E_{\mathrm{avg}} &+ \sum_{k=2,4,6} F^k f_k + \zeta_f A_{\mathrm{SO}} + \alpha L(L+1) \\ &+ \beta G(R_2) + \gamma G(R_7) + \sum_{i=2,3,4,6,7,8} T^i t_i \\ &+ \sum_{h=0,2,4} M^h m_h + \sum_{f=2,4,6} P^f p_f. \end{aligned} \tag{2}$$

There are up to 20 FI parameters in Eq. (2). The single-particle CF Hamiltonian is usually expressed in Wybourne's notation [17] in which the specific number of CF parameters is determined by site symmetry:

$$H_{\mathrm{CF}} = \sum_{k,q,i} B_{kq} C_{kq}(i). \tag{3}$$

The physical meaning of those FI parameters and CF parameters can be referred to Ref. [2] and references therein.

The lowest energy of the excited $4f^5 5d$ configuration is approximately 70,000 cm^{-1} higher than the ground level of the $4f^6$ configuration according to Dieke's FI spectra [18]. Specifically, among the trivalent lanthanide series, Eu^{3+} and Yb^{3+} have relatively large optical electronegativity thus much lower CTS due to the higher electron affinity of f^6 and f^{13} electronic configurations. For this reason, the CTS of Eu^{3+} or Yb^{3+} are generally much lower than the lowest energy levels of the $4f^5 5d$ configuration. Recently, van Pieterson et al. [19] reported a systematic study of CT luminescence from Yb^{3+}. Dorenbos [20] has summarized the systematic variation of trivalent lanthanide CT energies relative to the valence and conduction bands. The schematic diagram of energy-level structure as well as the CTS of Eu^{3+} is shown in Fig. 1. According to Jørgensen [21], the CTS position relative to the $4f^6$ ground state can be empirically estimated by

$$\Delta_{\mathrm{CT}} = [\chi(X) - \chi(\mathrm{Eu}^{3+})]3 \times 10^4\ \mathrm{cm}^{-1}, \tag{4}$$

where Δ_{CT} gives the position of CTS and $\chi(Eu^{3+})$ and $\chi(X)$ are the optical electronegativity of the Eu^{3+} ion and the ligand anion, respectively. For instance, the χ values have been determined to be about 1.75, 2.8, 3.2 and 3.9 for Eu^{3+}, S^{2-}, O^{2-} and F^-, respectively [21–23]. Therefore, the CTS position depends primarily on the nearest ligands in the host, and it may locate as high as 63,000 cm^{-1} for Eu^{3+}–F^- or as low as 28,000 cm^{-1} for Eu^{3+}–S^{2-}. Due to the much lower CTS, the *f–f* transitions of Eu^{3+} borrow the intensity according to Judd–Ofelt theory from the intermediate CTS instead of the $4f^5 5d$ states. This is achieved by mixing the $4f^6$ configuration with the CTS with the opposite parity via the interaction of odd CF or vibrational modes. As to be discussed later, the CTS play a very important role for the fluorescence intensity distribution of Eu^{3+}. On the other hand, the CTS play an important role also in the energy transfer and luminescence quenching processes of Eu^{3+} in some phosphors [24].

According to the branching ratios determined by the Judd–Ofelt theory, the transition from $^5D_0$ to $^7F_2$ is usually the strongest. It is hypersensitive to site symmetry and of electric-dipole (ED) nature. For comparison, the $^5D_0 \rightarrow {}^7F_1$ transition is primarily of magnetic-dipole (MD) nature and insensitive to site symmetry. The intensity ratio of the above transitions provides some structural information such as distortion of ligand environment and site symmetry. Radiative transitions to levels with $J=0$ or odd J ($J=3,5$) are both ED and MD forbidden, and only weak transitions from $^5D_0$ to these levels are observed due to CF-induced J-mixing effect.

Due to the large energy gap between the $^5D_0$ and $^7F_6$ ($\sim$12000 cm^{-1}) as shown in Fig. 1, the lifetime of $^5D_0$, usually on the order of milliseconds, does not vary significantly below room temperature (300 K). The

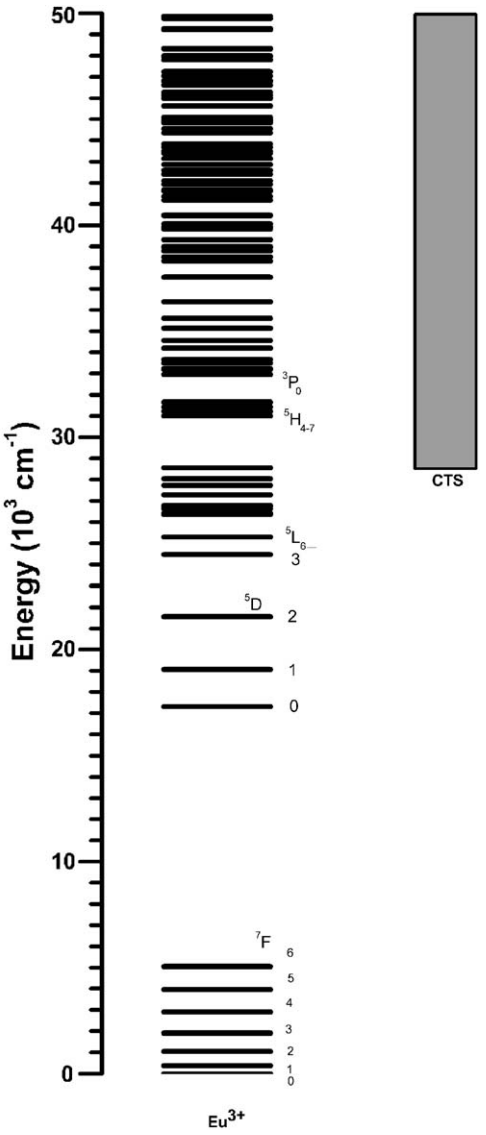

Fig. 1. The schematic diagram of energy-level structure as well as the CTS of Eu^{3+} ions in crystals.

fluorescence decay from $^5D_0$ of Eu^{3+} ions at normal sites is generally single exponential with an initial buildup time varying from μs to ms in different hosts due to nonradiative relaxation from $^5D_1$ and upper states.

CF spectra of Eu^{3+} in various crystals have been summarized in Table 1. The systems listed in Table 1 are grouped with similar compositions or structures for the purpose of a better comparison. For most of them, standard CF fitting has been carried out and the optimized CF parameters are available from the literatures listed in the last column. The value of Δ_{CT} is experimentally determined by the peak position of the lowest CT absorption band, and S is the scalar CF strength, according to Chang's definition [62]:

$$S = \left(\frac{1}{3}\sum_{k=2,4,6}\frac{1}{2k+1}\sum_{q}|B_{kq}|^2\right)^{1/2}. \quad (5)$$

Note that S can be converted to N_v, another CF strength defined by Auzel et al. [63,64] by: $N_v = \sqrt{12\pi}S \approx 6S$. I_{00}/I_{01} is the ratio of the integrated intensity of $^5D_0 \rightarrow {}^7F_0$ to $^5D_0 \rightarrow {}^7F_1$, an important factor that indicates the behavior of the Eu^{3+} fluorescence dynamics. According to the ED selection rule, 0–0 transitions are only allowed in the following 10 site symmetries, C_s, C_1, C_2, C_3, C_4, C_6, C_{2v}, C_{3v}, C_{4v}, and C_{6v}, because there exist linear CF components. As shown in Table 1, for those standard CF spectra, the 0–0 transition is very weak. Also tabulated in Table 1, the lifetime of $^5D_0$ varies from several hundred microseconds to 10 ms depending on the type of hosts.

Some useful inferences can be obtained based on the comparison of hosts that belong to the same or different families. First, the lifetime of $^5D_0$ is generally much longer in halide hosts than in oxide or oxysulfide hosts due to much higher CTS in the former. Similar to the case of $4f^5 5d$ intermediate states, the radiative lifetime of $^5D_0$ is approximately proportional to the square of Δ_{CT}, as can be derived from the second-order ED transition mechanism in the Judd–Ofelt theory. One should keep in mind that the above lifetime variation cannot be ascribed to any multi-phonon relaxation mechanism since the maximum phonon frequency in those solids is very low ($<1000\,cm^{-1}$) compared to the large energy gap; therefore, the nonradiative relaxation rate is negligibly small. Secondly, the shift of Δ_{CT} to lower energies in the series of Lu, Y, Gd, La (such as Ln_2O_2S and $LnOX$, Ln = lanthanide, X = halide) can be ascribed to the larger cation radius, which results in a lower Madelung potential at the anion sites, as pointed out by Blasse [65]. On the other hand, the shift of Δ_{CT} to lower energies in the series of F, Cl, Br, I, (such as LaX_3 and $LnOX$) is mainly due to the smaller optical electronegativity along this series, which results in the nephelauxetic (electron cloud expanding) effect. Thirdly, contrary to Δ_{CT}, no consistent trends for the variation of the CF strength along the series can be found. For example, as shown in Table 1, the CF strength decreases with increasing ionic radius of the host cation for the Ln_2O_2S family. This evolution is the reverse of that for the $LnOX$ families. In fact, many factors such as ionic radii, optical electronegativity, covalency, and structural distortion could significantly influence the CF interaction of the Eu^{3+} ion.

3.2. Anomalous CF spectra of Eu^{3+}

Since the ratio of I_{00}/I_{01} can be used as a probe of fluorescence dynamics of Eu^{3+}, Table 1 also lists some

Table 1
A summary of crystal-field spectra of Eu^{3+} in different crystals

Host	Site symmetry	S (cm^{-1})	Δ_{CT} ($\times 10^3\,cm^{-1}$)	I_{00}/I_{01}	$\tau(^5D_0)$ (ms)	Ref.
Lu_2O_3	C_2	718	40.5	0.15	1.00	[25,26]
Y_2O_3	C_2	673	40.8	0.15	0.90	[27,28]
Lu_2O_2S	C_{3v}	395	~30.0	~0.3	0.59	[20,29,30]
Y_2O_2S	C_{3v}	375	29.0	0.3	0.44	[20,29–31]
Gd_2O_2S	C_{3v}	361	~29.0	~0.3	0.41	[20,29,30]
La_2O_2S	C_{3v}	314	~28.8	~0.3	0.37	[20,29,30]
YOCl	C_{4v}	395	35.4	0.5	—[a]	[5,6]
GdOCl	C_{4v}	398	35.0	0.4	—	[5,6]
LaOCl	C_{4v}	460	33.3	2 (second strongest)	—	[5,6]
YOBr	C_{4v}	426	33.9	<0.1	—	[7]
GdOBr	C_{4v}	440	33.4	0.2	—	[7]
LaOBr	C_{4v}	513	32.9	2.5 (strongest)	—	[7]
LaOI	C_{4v}	515	29.8	—	—	[7,20]
$LaONO_3$	C_{2v}	467	—	0.6	—	[9]
YPO_4	D_{2d}	247	45.0	0	0.25	[24,32,33]
YVO_4	D_{2d}	250	31.2	0	0.475	[24,32,34]
$LaPO_4$	$C_1(\sim C_{2v})$[b]	317	37.0	0.01	4.27	[24,35,36]
$LaVO_4$	$C_1(\sim C_{2v})$[b]	428	~30.0	0.02	—	[24,35]
$LaBO_3$	C_{2v}	438	44.4	0.02	—	[20,37,38]
EuP_5O_{14}	$C_1(\sim C_{2v})$[b]	318	—	<0.01	5.0	[39,40]
$YAlO_3$	C_s	464	~39.0	<0.02	1.64	[41]
$LaAlO_3$	D_3	440	32.0	0	2.0	[42,43]
$YAl_3(BO_3)_4$	D_3	497	—	0	1.14	[44,45]
$GdAl_3(BO_3)_4$	D_3	402	39.4	0	1.16	[20,44,46]
$Y_3Al_5O_{12}$	D_2	682	44.7	0	4.00	[47–49]
$Y_3Ga_5O_{12}$	D_2	484	42.6	0	—	[20,50]
LaF_3	C_{2v}	346	~63.0	0.05	6.70	[2,51]
$LaCl_3$	C_{3h}	192	~41.5	0	—	[52]
$LiYF_4$	S_4	379	~63.0	0	—	[53,54]
KY_3F_{10}	C_{4v}	323	~63.0	~0	5.80	[55]
Cs_2NaYCl_6	O_h	498	~41.5	0	11.1	[56,57]
$Cs_2NaEuCl_6$	O_h	536	~41.5	0	5.50	[56,57]
ThO_2	C_{3v}	589	39.5	0.1	0.86	[58]
	O_h	748	39.5	<0.01	5.27	[58]
CaF_2	$C_{4v}(F^-)$[c]	475	66.0	—	11.8	[20,59]
	$C_{3v}(O^{2-}$, G1)[d]	Large	~42.0	2.7 (second strongest)	1.81	[60]
$Sr_5(PO_4)_3F$	$C_s(O^{2-})$[e]	Large	~32.5	>20 (strongest)	—	[13]
$Ca_{10}(PO_4)_6(OH)_2$	$C_s(O^{2-})$[f]	Large	31.4	~10 (strongest)	0.52	[61]
$Ca_{10}(PO_4)_6(OH)_2$:BO_3^{3-}	$C_s(O^{2-})$[f]	Large	32.3	~10 (strongest)	0.58	[61]
BaFCl	C_{2v}	538	41.5	0.058	0.78	This work
	$C_s(O^{2-})$[g]	Large	35.0	25 (strongest)	0.31	This work

[a]Not available.
[b]The site symmetry is approximately taken as C_{2v} in the CF fitting.
[c]Charge-compensating fluoride ion located in an interstitial position along the [100] direction.
[d]Charge-compensating oxide ion substituting a nearest-neighbor fluoride ion in the lattice along the [111] direction, usually labeled as G1 center in CaF_2 crystals.
[e]Eu^{3+} in the Sr(II) site, charge-compensating oxide ion substituting a nearest-neighbor fluoride ion in the lattice.
[f]Eu^{3+} in the Ca(II) site (6*h* site), charge-compensating oxide ion substituting a nearest-neighbor OH^- group in the lattice.
[g]Charge-compensating oxide ion substituting a nearest-neighbor fluoride ion in the lattice.

anomalous Eu^{3+} containing systems where "strongest" or "second strongest" is marked in the I_{00}/I_{01} column. For instance, the $^5D_0 \rightarrow {}^7F_0$ line was observed to be the strongest among those transitions from the same $^5D_0$ state in Eu^{3+}:LaOBr [7]. As we know, the extent of CF mixing of a state with different J should be no more

than 10% of the total wave function. Obviously, it is impossible for such a low extent of J-mixing to induce the strongest $^5D_0 \rightarrow {}^7F_0$ line. It is obvious that the role of CF J-mixing has been overestimated in the previous work in which strong $^5D_0 \rightarrow {}^7F_0$ line was reported [7–8,13].

It was realized by Nieuwpoort and Blasse [4] and Judd [66] in 1966 that the linear CF parameters which exist only in particular site symmetries may play an important role in inducing the strong 0–0 transition as well as the hypersensitive 0–2 transition. To resolve this puzzle, Wybourne [67] and Downer et al. [68,69] later proposed a mechanism of spin–orbit interaction in the excited-state configuration to include the third-order ED contribution that was previously neglected in calculating the electronic transition intensity. Their work was actually an extension of the Judd–Ofelt theory. Similar to the derivation by Downer et al. [68], a semi-quantitative expression of the line intensity of 0–0 transition can be derived by taking into account the intermediate CTS

$$I(^5D_0 \rightarrow {}^7F_0) \propto \frac{S_1^2}{\Delta_{CT}^4}, \tag{6}$$

$$S_1 = \left(\frac{1}{3} \sum_{q=0,\pm 1} |A_{1q}|^2 \right)^{1/2}, \tag{7}$$

where S_1 is the scalar linear CF rotational invariant and A_{1q} is the linear CF components. Therefore, the presence of even a small linear CF term in the CF Hamiltonian could contribute a large enhancement to the strength of the $^5D_0 \rightarrow {}^7F_0$ transition in those systems where the energy gap between CTS and the $4f$ states is relatively small.

Several interesting features should be noted in Table 1. (1) Anomalous CF spectra are often found in those systems in which the charge is not balanced (such as Eu^{3+} substituting Ca^{2+}), and particularly there are oxygen-compensating sites. This observation indicates the strong CT-induced lattice distortion [70,71]. The influence of lattice distortion in those systems can be understood as the following. In a CT process, the trivalent Eu is virtually reduced to divalent Eu with a hole left in the ligand, and the ionic radius will be increased from 98 to 116 pm [20]. Obviously, this process will be followed by a strong lattice relaxation. (2) The hosts with anomalous CF spectra usually have a very large CF strength, and the standard CF fitting program often fails to fit their energy levels. To improve the fit for anomalous CF spectra, the effects of covalency and delocalization of f-electron on the Eu^{3+} CF might have to be reconsidered, in view of the complicated chemical nature of CT process in those charge-unbalanced systems.

4. CF spectra of Eu^{3+}:BaFCL microcrystals

We now discuss the spectroscopic properties of two main sites of Eu^{3+} in BaFCl microcrystals. Special emphasis will be given to the spectroscopic comparison between the normal site (Site I) and anomalous site (Site II).

Because of charge imbalance and the presence of point defects, multiple sites are expected for trivalent Eu^{3+} ions in BaFCl crystals. Previous studies on Eu^{3+}-doped bulk BaFCl crystal [72,73] have identified the existence of more than 15 sites (see Fig. 1 in Ref. [73]) and demonstrated laser-excitation-induced Eu^{3+} site-to-site conversion for persistent spectral hole burning. Based on the charge-transfer vibronic exciton (CTVE) model in charge-unbalanced solids, Vikhnin et al. [70,71] have explained the mechanism of multi-site structure conversion. That is, the CTVE clusters trapped by charged impurities (Eu^{3+} in Ba^{2+} site of BaFCl) are likely connected with different sites as detected in the spectroscopic experiments. As shown in Fig. 2, when pumped by a laser in UV region, multi-site structures in Eu^{3+}:BaFCl microcrystals were verified. The main site of Eu^{3+} was determined to be Site I for laser pumping at

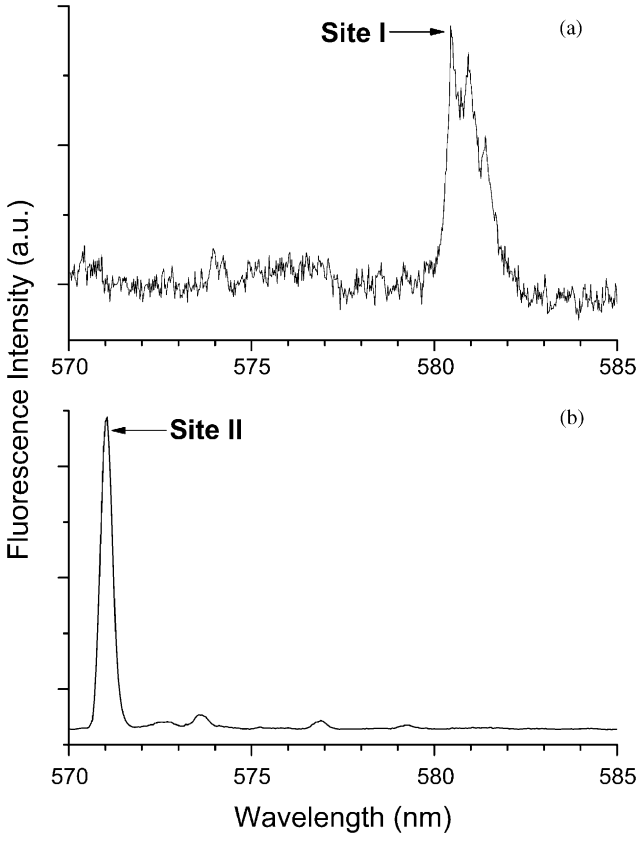

Fig. 2. Fluorescence spectra in the region of $^5D_0 \rightarrow {}^7F_0$ for Eu^{3+}:BaFCl microcrystals under UV excitation at (a) 266 nm; and (b) 355 nm. Both spectra were measured at 4 K.

266 nm, and Site II for laser pumping at 355 nm. It should be noted that the observed multi-site structure in the microcrystals is very different from that in the bulk counterparts due to the role of oxygen defect in the former. For instance, Sites I or II are not the main sites in the bulk unoxidized crystals when pumped by a 355 nm laser. But, after aging this bulk sample in the air for a long time, its multi-site structure becomes very similar to that of the microcrystals. Sites I and II can be selectively excited to $^5D_1$ by a dye laser at 526.85 and 553.62 nm, respectively. The fluorescence spectra of Sites I and II in the range of 570–850 nm which corresponds to the $^5D_0 \rightarrow {}^7F_J$ ($J = 0 - 6$) transitions are compared in Figs. 3(a–c), respectively. The energy levels of both sites are summarized in Table 2.

4.1. Site I

As shown in Fig. 3 and Table 2, the fluorescence intensity distribution and CF splitting of Eu^{3+} at Site I in BaFCl are similar to the most cases reported hitherto. In those cases, the strongest transition occurs between $^5D_0$ and $^7F_2$ and the $^5D_0 \rightarrow {}^7F_0$ transition is very weak. Based on such a comparison, we assume that a Eu^{3+} ion at Site I substitutes the Ba^{2+} site at an approximate C_{4v} symmetry in the lattice. Actually, the CF environment of the Eu^{3+} may be distorted toward C_{2v} due to the charge imbalance around the Eu^{3+}. This reduced site symmetry has been further confirmed by the number of allowed CF transitions identified from unpolarized emission spectra at low temperature. Were the site symmetry of Site I exactly C_{4v}, according to the selection rules, the allowed maximum CF transitions due to the forced ED or MD nature from $^5D_0$ to ^7F_J would be 2 ($J = 1$), 2 ($J = 2$), 2 ($J = 3$), 4 ($J = 4$), 4 ($J = 5$) and 5 ($J = 6$), respectively, which would show less fluorescence peaks than in the observed unpolarized emission spectra.

Based on a C_{2v} site symmetry, we have performed the energy-level analysis and standard CF fitting for Site I by using the method discussed in Section 3.1. The final FI and CF parameters are listed in Table 3. It is not possible to label the CF levels with irreducible representations from unpolarized measurements on microcrystals. Therefore, for those multiplets to which incomplete CF levels were assigned, the experimental CF levels were assigned to the energetically closest calculated ones. The initial values of the FI parameters were taken from Carnall et al. [2], while initial values of the CF parameters were estimated based on the modified point-charge model and lattice-sum technique [1]. The rms deviation (23 cm^{-1}) is a little bit larger than other hosts reported in Table 1. The relatively small values of B_{42}, B_{62}, and B_{66} obtained are in accordance with the hypothesis that the site symmetry is slightly distorted from C_{4v}. It is worthy to mention that the ratios of CF parameters with the same rank for

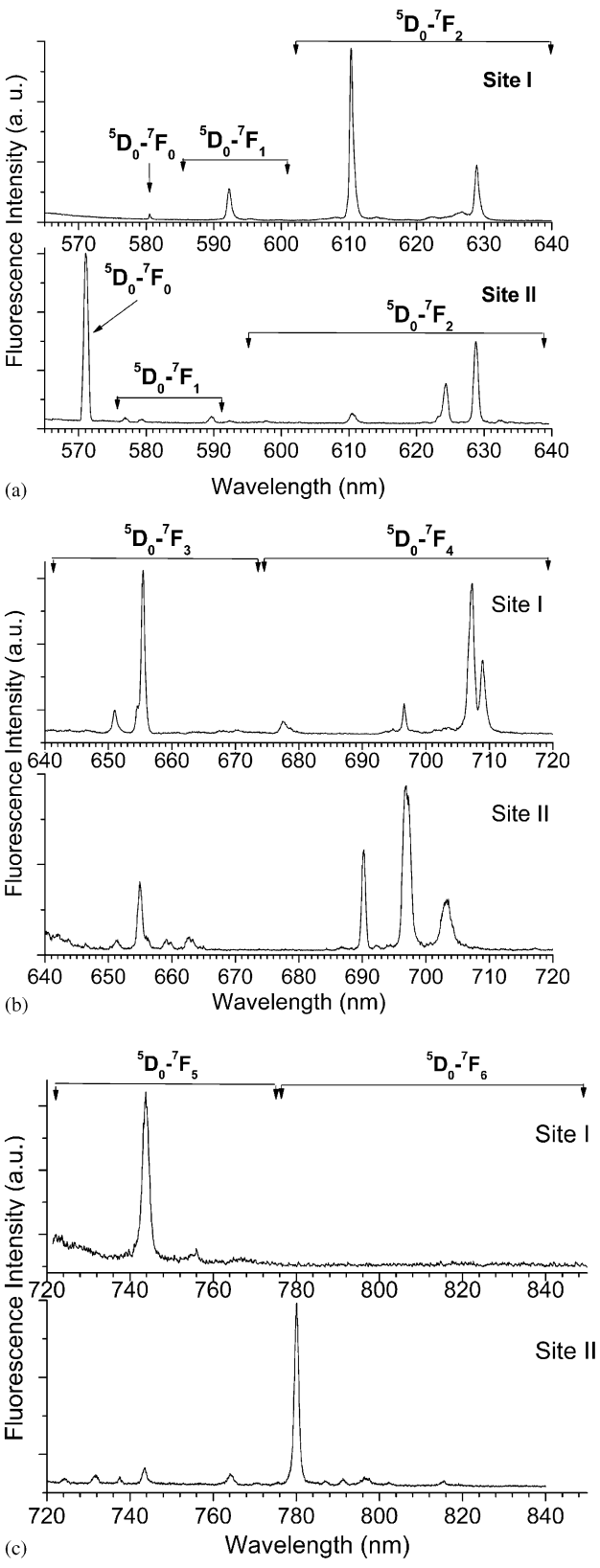

Fig. 3. Comparison of fluorescence spectra of Eu^{3+}:BaFCl microcrystals at Sites I and II in the range of (a) 570–640 nm; (b) 640–720 nm; and (c) 720–850 nm, site-selectively excited by dye laser at 3.2 K. The fluorescence emission was detected using a boxcar integrator that averaged the fluorescence signal from a cooled PMT with 15 μs gate width. The delays from the pump laser pulse were set at 0.10 and 0.23 ms for Sites I and II, respectively.

Table 2
The energy levels of Eu^{3+} at two main sites in BaFCl microcrystals at 3 K

Multiplet	Site I		Site II
	Exp (cm^{-1})	Fit (cm^{-1})	Exp (cm^{-1})
$^7F_0$	0	1	0
$^7F_1$	293	290	176
	343	355	249
	432	450	549
$^7F_2$	781	828	780
	842	837	1145
	942	912	1494
	1271	1234	1607
	1326	1302	1699
$^7F_3$	—	1824	1929
	1865	1844	1966
	—	1917	2154
	—	1942	2237
	1948	1951	2330
	1970	1970	2348
	—	2111	2411
$^4F_4$	2466	2461	3018
	2811	2803	3064
	2834	2835	3099
	2871	2866	3150
	2975	2985	3164
	3013	3021	3206
	3080	3088	3270
	3089	3112	3283
	3121	3141	3292
$^7F_5$	—	3752	3700
	—	3754	3843
	3782	3781	3954
	—	3878	4063
	3977	3970	4426
	4000	3979	
	—	4058	
	—	4061	
	—	4143	
	4194	4208	
	—	4217	
$^7F_6$	—	4885	4694
	—	4891	4806
	—	5006	4874
	—	5010	4952
	—	5085	4979
	—	5092	5049
	—	5093	5247
	—	5174	
	—	5181	
	—	5255	
	—	5257	
	—	5258	
	—	5259	
$^5D_0$	17227	17236	17512
$^5D_1$	18981	18971	18063
	—	18992	
	—	19015	

Table 3
FI and CF parameters (in cm^{-1}) for Site I of Eu^{3+}:BaFCl in approximate C_{2v} symmetry

Parameter[a]	Fitted values[b]
E_{avg}	63768(77)
F^2	82638(102)
F^4	[60937]
F^6	[41121]
ξ	1318(5)
B_{20}	−72(75)
B_{22}	−290(52)
B_{40}	−1489(96)
B_{42}	188(183)
B_{44}	1266(70)
B_{60}	16(145)
B_{62}	51(98)
B_{64}	1200(66)
B_{66}	−101(125)
rms[c]	23

[a]The α, β, γ, T^i ($i = 2, 3, 4, 6, 7, 8$), M^j ($j = 0, 2, 4$), and P^k ($k = 2, 4, 6$) parameters were kept constant during the fitting procedure at the following values [2]: $\alpha = 20.16$, $\beta = -566.9$, $\gamma = 1500$; $T^2 = 300$, $T^3 = 40$, $T^4 = 60$, $T^6 = -300$, $T^7 = 370$, $T^8 = 320$; $M^0 = 2.1$, $M^2/M^0 = 0.56$, $M^4/M^0 = 0.31$; $P^2 = 360$, $P^4/P^2 = 0.5$, $P^6/P^2 = 0.1$.

[b]Values in parentheses are errors in the indicated parameters. Values in brackets were not allowed to vary in the parameter fitting.

[c]Deviation $rms = \Sigma[(\Delta i)^2/n\text{-}p]^{1/2}$, where Δi is the difference between observed and calculated energies, n is the number of levels fit, and p is the number of parameters freely varied.

Eu^{3+}:BaFCl (B_{44}/B_{40} and B_{64}/B_{60}) are different from those available for Sm^{2+}:BaFCl [74,75] although the Sm^{2+} ion is isoelectronic to Eu^{3+}. It is understood since the local environment distortion of Eu^{3+} caused by the charge imbalance in BaFCl may strongly influence those structural parameter ratios. In fact, the signs of the resulting CF parameters for Site I are in agreement with those calculated ones which include the contributions of point charges, dipoles and quadrupoles [76].

Interestingly, an "anomaly" in the fluorescence intensity pattern of Site I is observed in Fig. 3(b). The usually weak $^5D_0 \rightarrow {}^7F_3$ line at 655.4 nm is even stronger than the strongest line among $^5D_0 \rightarrow {}^7F_4$ transitions (Fig. 3(b)). This "anomaly" can be well explained by CF-induced J-mixing. The wave function of the CF levels obtained from CF analysis showed clearly that J-mixing from $^7F_2$ to $^7F_3$ induced by the large fourth-rank CF parameters ($B_{40} = -1489\,cm^{-1}$ and $B_{44} = 1266\,cm^{-1}$) can reach as high as 6.5%, thus contributing significantly to the strong $^5D_0 \rightarrow {}^7F_3$ line. For comparison, the extent of J-mixing from $^7F_2$ to $^7F_0$ is about 2%, induced by the relatively small second rank CF parameters ($B_{20} = -72\,cm^{-1}$ and $B_{22} = -290\,cm^{-1}$). This result is in accordance with the observed weak intensity of the $^5D_0 \rightarrow {}^7F_0$ line in Fig. 3(a).

4.2. Site II

As for Eu^{3+} ions at Site II, the fluorescence intensity distribution is quite different. The strongest $^5D_0 \rightarrow {}^7F_0$ and second strongest $^5D_0 \rightarrow {}^7F_2$ transitions (Fig. 3(a)) cannot simply be ascribed to *J*-mixing effect. Moreover, as shown in Fig. 3(c), a very strong $^5D_0 \rightarrow {}^7F_6$ emission at 780 nm comparable to the $^5D_0 \rightarrow {}^7F_4$ intensity is observed for Site II, whereas this transition is too weak to be observed for Site I. The unusually high position of the $^5D_0$ level (17512 cm^{-1}) exceeds most of the values reported for other Eu^{3+}-doped crystalline compounds. Similar to our observations, Piriou et al. [8] observed the high position of the $^5D_0$ level (17450 cm^{-1} for *A* site and 17,510 for *B* site) in $Ca_{10-x}Eu_x(PO_4)_6O_{1+x/2}$ polycrystallines. Wright et al. [13] also observed the high position of the $^5D_0$ level (17,525 cm^{-1} and 17,550 for two sites) in $Sr_5(PO_4)_3F$ single crystals. In an early report, Gaigerova et al. [77] suggested that CTS should be responsible for the high-energy position and the high intensity of $^5D_0 \rightarrow {}^7F_0$ line observed in several charge-unbalanced matrices.

The $^5D_1$ level of Eu^{3+} at Site II is located at an unusual low position (18063 cm^{-1}) in comparison with the range of 18,900–19,100 cm^{-1} for Eu^{3+} in most crystals. As a result, the energy gap between $^5D_1$ and $^5D_0$ reduces to only 551 cm^{-1}. Such a narrow energy gap has never been reported in other charge-unbalanced systems such as oxyapatite or strontium fluorapatite aforementioned. Due to the large CF parameters, the CF-level splitting of $^7F_2$ at Site II was observed to be as wide as 919 cm^{-1}. Similar CF splitting of $^7F_2$ was previously reported for the oxyapatite or strontium fluorapatite systems [8,13,78].

Our spectroscopic results indicate that the CF environment of Eu^{3+} at Site II is strongly distorted. Most importantly, for Site II, the inevitable oxygen defects act as the charge compensator of Eu^{3+} by substituting the nearest F^-. The symmetry of Site II is presumably reduced to C_s. Our results suggest that Site II is dominant in the microcrystals, and in the aged bulk crystals as well, possibly due to the increasing oxygen defects [79]. Currently, attempts to perform the CF-level fitting of Eu^{3+} at Site II by the same diagonalization approach as we did for Site I does not result in good agreement between the experimental data and calculations. This also happened in some other Eu-doped charge-unbalanced systems, such as $Sr_5(PO_4)_3F$ [13]. It is possibly due to (1) drastic changes in the electronic states of Eu^{3+} at Site II in consistency with the large line shifts; (2) inaccurate energy-level assignment because of the lines due to other indistinguishable sites; and (3) the failure of the standard CF model as discussed in Section 3.2. Further work on the CF analysis of Site II to include the covalency or RE delocalization effects may improve the fitting. However, in comparison with the CF splittings at Site I, the CF strength of Site II is obviously much larger than that of Site I. By utilizing Leavitt's method [80], the CF strength of Site II has been roughly estimated to be about 1300 cm^{-1} according to the fitting of CF invariant (rank 2, 4, and 6) on the three reliable ^7F_J ($J = 1, 2, 3$) multiplets.

4.3. Fluorescence lifetime

Fluorescence decay of the $^5D_0$ state of Eu^{3+}:BaFCl microcrystals at different temperatures for both sites was measured and compared. The detailed discussion on the mechanisms of efficient energy-transfer processes for Eu^{3+} at both sites in the diluted BaFCl microcrystals is beyond the scope of the present paper and will be presented elsewhere [79]. To support the present analysis of CF spectra, it is noteworthy to mention the following facts: (1) The fluorescence decay curves of Eu^{3+} at Site I at all temperatures are significantly nonexponential, whereas the decays for Eu^{3+} at Site II are perfectly single exponential from 3 up to 180 K. The fluorescence decays of Eu^{3+} at both sites are sensitive to temperature with no rise time, which is contrary to the normal Eu^{3+} decay characteristics of $^5D_0$. (2) The measured radiative lifetime of Eu^{3+} at Site I is 0.779 ms. The rate of energy transfer from the Eu^{3+} at Site I to the acceptors or traps (e.g. Eu^{3+} in other sites, self-trapped exciton, and surface defect) obeys approximately T^2 dependence on temperature. (3) The measured radiative lifetime of Eu^{3+} at Site II is 0.305 ms. The temperature dependence of nonradiative energy transfer rates for Eu^{3+} at Site II is observed to obey an approximately T^9 dependence which is quite unusual for Eu^{3+} in dielectric crystals. It is expected that, the lower CTS and larger linear CF parameters of Eu^{3+} at Site II may lead to the shorter radiative lifetime of $^5D_0$ than that of Site I.

5. Conclusions

We have analyzed the CF spectra of Eu^{3+} in terms of standard and anomalous behaviors. Results from Eu^{3+}:BaFCl crystals have been interpreted based on CF theory and various mechanisms of electronic transitions. Comparison is made with previous results for Eu^{3+} in inorganic crystalline hosts. Unlike other RE ions in the series, Eu^{3+} has much lower CTS. In addition to the 5*d* states, the CTS with opposite parity may act as the intermediate state to induce the second-order ED (Judd–Ofelt mechanism) and third-order ED (Wybourne–Downer mechanism) transitions. Whereas one of the Eu^{3+} site has normal characteristics that can be interpreted by the standard CF model, the anomalous CF spectra and fluorescence dynamics of Eu^{3+} at another site are attributed to charge imbalance and specifically to oxygen compensators that induce strong

CF distortion. In such an anomalous CF environment, a third-order ED contribution should be comparable to or even larger than that from the second-order ED. Evidently, the fluorescence spectra and dynamics of Eu^{3+} in charge-unbalanced solids are significantly influenced by the electron transfer process (covalency) and *f* electron delocalization.

Due to the strong distortion of CF environment and a large linear CF terms enhanced by charge-imbalance, Eu^{3+} ions at Site II not only exhibit distinct fluorescence intensity distribution and line-shifts but also have unusual temperature-sensitive lifetime. We believe that these anomalous fluorescence properties can be well described within the framework of Wybourne–Downer mechanism. However, there are still some theoretical difficulties to quantitatively evaluate the Wybourne–Downer mechanism for Eu^{3+} systems which includes the nonlocal CTS. From this point of view, fundamental understanding of the Wybourne–Downer mechanism enhanced by charge-imbalance or covalency is of great importance to gain more insights into the physical or chemical nature of lanthanide spectra.

Acknowledgments

Work at Argonne National Laboratory was performed under the auspices of the Office of Basic Energy Science, Division of Chemical Sciences, US Department of Energy, under Contract No. W-31-109-ENG-38. The authors are grateful to Wei Zhao for providing them the Eu^3:BaFCl samples and to R.E. Cook for TEM images. The authors are also grateful to M.F. Reid for the use of *f*-shell empirical program and to B.Z. Malkin and V.S. Vikhnin for helpful discussion.

References

[1] C.A. Morrison, R.P. Leavitt, in: K.A. Gschneidner, L. Eyring (Eds.), Handbook on the Physics and Chemistry of Rare Earths, vol. 5, North-Holland, Amsterdam, 1982, p. 584 (Chapter 46).
[2] W.T. Carnall, G.L. Goodman, K. Rajnak, R.S. Rana, J. Chem. Phys. 90 (1989) 3443.
[3] C. Gorller-Warland, K. Binnemans, in: K.A. Gschneidner, L. Eyring (Eds.), Handbook on the Physics and Chemistry of Rare Earths, vol. 23, North-Holland, Amsterdam, 1996, p. 121 (Chapter 155); vol. 25, North-Holland, Amsterdam, 1998, p. 101 (Chapter 167).
[4] W.C. Nieuwpoort, G. Blasse, Solid State Commun. 4 (1966) 227.
[5] G. Blasse, A. Bril, J. Chem. Phys. 46 (1967) 2579.
[6] J. Holsa, P. Porcher, J. Chem. Phys. 75 (1981) 2108.
[7] J. Holsa, P. Porcher, J. Chem. Phys. 76 (1982) 2790.
[8] B. Piriou, D. Fahmi, J. Dexpert-Ghys, A. Taitai, J.L. Lacout, J. Lumin. 39 (1987) 97.
[9] J. Holsa, M. Karppinen, Eur. J. Solid State Inorg. Chem. 28 (1991) 135.
[10] D. Zakaria, R. Machiou, D. Zambon, M.T. Fournier, Eur. J. Solid State Inorg. Chem. 28 (1991) 109.
[11] N.J. Cockroft, S.H. Lee, J.C. Wright, Phys. Rev. B 44 (1991) 4117.
[12] A. Zounani, D. Zambon, J.C. Cousseins, J. Alloys Compd. 207–208 (1994) 94.
[13] A.O. Wright, M.D. Seltzer, J.B. Gruber, B.H.T. Chai, J. Appl. Phys. 78 (1995) 2456.
[14] B.R. Judd, Phys. Rev. 127 (1962) 750.
[15] G.S. Ofelt, J. Chem. Phys. 37 (1962) 511.
[16] J.C.G. Bunzli, G.O. Pradervand, J. Chem. Phys. 85 (1986) 2489.
[17] B.G. Wybourne, Spectroscopic Properties of Rare Earths, Wiley Interscience, New York, 1965.
[18] G.H. Dieke, in: H.M. Crosswhite, H. Crosswhite (Eds.), Spectra and Energy Levels of Rare Earth Ions in Crystals, Interscience, New York, 1968.
[19] L. van Pieterson, M. Heeroma, E. de Heer, A. Meijerink, J. Lumin. 91 (2000) 177.
[20] P. Dorenbos, J. Phys.: Condens. Matter 15 (2003) 8417.
[21] C.K. Jørgensen, Modern Aspects of Ligand-Field Theory, North-Holland, Amsterdam, 1971 (Chapter 28).
[22] N. Vugt, T. Wigmans, G. Blasse, J. Inorg. Nucl. Chem. 35 (1973) 2602.
[23] C.K. Jørgensen, Mol. Phys. 5 (1962) 271.
[24] G. Blasse, Struct. Bonding 26 (1976) 43.
[25] M. Karbowiak, E. Zych, J. Holsa, J. Phys.: Condens. Matter 15 (2003) 2169.
[26] E. Zych, J. Phys.: Condens. Matter 14 (2002) 5637.
[27] M.J. Weber, Phys. Rev. 171 (1968) 283.
[28] R.P. Leavitt, J.B. Gruber, N.C. Chang, C.A. Morrison, J. Chem. Phys. 76 (1982) 4775.
[29] O.J. Sovers, T. Yoshioka, J. Chem. Phys. 51 (1969) 5330.
[30] T. Hoshina, S. Imanaga, S. Yokono, J. Lumin. 15 (1977) 455.
[31] G. Nishimura, M. Tanaka, A. Kurita, T. Kushida, J. Lumin. 48&49 (1991) 473.
[32] C. Linares, A. Louat, M. Blanchard, Struct. Bonding 33 (1977) 179.
[33] W.W. Moses, M.J. Weber, S.E. Perenzo, D. Perry, P. Berdahl, L.A. Boatner, IEEE Trans. Nucl. Sci. NS-45 (1998) 462.
[34] G.E. Venikouas, R.C. Powell, J. Lumin. 16 (1978) 28.
[35] E. Antic-Fidancev, J. Holma, M. Lemaitre-Blaise, P. Porcher, J. Phys.: Condens. Matter 3 (1991) 6829.
[36] M. Yu, J. Lin, J. Fu, H.J. Zhang, Y.C. Han, J. Mater. Chem. 13 (2003) 1413.
[37] J.A. Capobianco, P.P. Proulx, N. Raspa, D.J. Simkin, D. Krashkevich, J. Chem. Phys. 90 (1989) 2856.
[38] H. Giesber, J. Ballato, G. Chumanov, J. Kolis, M. Dejneva, J. Appl. Phys. 93 (2003) 8987.
[39] C. Brecher, J. Chem. Phys. 61 (1974) 2297.
[40] R.M. Macfarlane, R.M. Shellby, in: A.A. Kaplyanskii, R.M. Macfarlane (Eds.), Spectroscopy of Solids Containing Rare Earth Ions, North-Holland, Amsterdam, 1987, p. 51.
[41] X.Y. Chen, G.K. Liu, Unpublished results.
[42] G. Blasse, A. Bril, J.A. de Poorter, J. Chem. Phys. 53 (1970) 4450.
[43] D. Garcia, M. Faucher, J. Chem. Phys. 82 (1985) 5554.
[44] F. Kellendonk, G. Blasse, J. Chem. Phys. 75 (1981) 561.
[45] C. Gorller-Warland, P. Vandevelde, I. Hendrickx, P. Porcher, J.C. Krupa, G.S.D. King, Inorg. Chim. Acta 143 (1988) 259.
[46] C. Gorller-Warland, E. Huygen, K. Binnemans, L. Fluyt, J. Phys.: Condens. Matter 6 (1994) 7797.
[47] H. Gross, J. Neukum, J. Heber, D. Mateika, T. Xiao, Phys. Rev. B 48 (1993) 9264.
[48] K. Binnemans, C. Gorller-Walrand, J. Chem. Soc. Faraday Trans. 92 (1996) 2487.
[49] W.T. Hsu, W.H. Wu, C.H. Lu, Mater. Sci. Eng. B 104 (2003) 40.
[50] J.A. Koningstein, J. Chem. Phys. 42 (1965) 3195.

[51] M.J. Weber, in: H.M. Crosswhite, H.W. Moos (Eds.), Optical Properties of Ions in Crystals, Wiley Interscience, New York, 1967, p. 467.
[52] C.K. Jayasankar, F.S. Richardson, M.F. Reid, J. Less-Common Met. 148 (1989) 289.
[53] C. Gorller-Warland, M. Behets, P. Porcher, W.T. Carnall, Inorg. Chim. Acta 126 (1986) 271.
[54] C. Gorller-Warland, K. Binnemans, L. Fluyt, J. Phys.: Condens. Matter 5 (1993) 8359.
[55] P. Porcher, P. Caro, J. Chem. Phys. 65 (1976) 89.
[56] P.A. Tanner, V.V.R.K. Kumar, C.K. Jayasankar, M.F. Reid, J. Alloys Compd. 225 (1995) 85.
[57] M. Bettinelli, C.D. Flint, J. Phys.: Condens. Matter 3 (1991) 7053.
[58] M. Yin, J.C. Krupa, E. Antic-Fidancev, A. Lorriaux-Rubbens, Phys. Rev. B 61 (2000) 8073.
[59] J.P.R. Wells, R.J. Reeves, Phys. Rev. B 64 (2001) 035102.
[60] F.J. Gustafson, J.C. Wright, Anal. Chem. 51 (1979) 1762.
[61] R. Ternane, G. Panczer, M.Th. Cohen-Adad, C. Goutaudier, G. Boulon, N. Kbir-Ariguib, M. Trabelsi-Ayedi, Opt. Mater. 16 (2001) 291.
[62] N.C. Chang, J.B. Gruber, R.P. Leavitt, C.A. Morrison, J. Chem. Phys. 76 (1982) 3877.
[63] F. Auzel, Mater. Res. Bull. 14 (1979) 223.
[64] F. Auzel, O.L. Malta, J. Phys. (France) 44 (1983) 201.
[65] G. Blasse, J. Chem. Phys. 45 (1966) 2356.
[66] B.R. Judd, J. Chem. Phys. 44 (1966) 839.
[67] B.G. Wybourne, in: H.M. Crosswhite, H.W. Moos (Eds.), Optical Properties of Ions in Crystals, Wiley Interscience, New York, 1967, p. 35;
B.G. Wybourne, J. Chem. Phys. 48 (1968) 2596;
B.G. Wybourne, Eur. J. Solid State Inorg. Chem. 28 (1991) 19.
[68] M.C. Downer, G.W. Burdick, D.K. Sardar, J. Chem. Phys. 89 (1988) 1787.
[69] G.W. Burdick, M.C. Downer, D.K. Sardar, J. Chem. Phys. 91 (1989) 1511.
[70] V.S. Vikhnin, G.K. Liu, J.V. Beitz, Phys. Lett. A 287 (2001) 419.
[71] V.S. Vikhnin, A.A. Kaplyanskii, A.B. Kutsenso, G.K. Liu, J.V. Beitz, S.E. Kapphan, J. Lumin. 94–95 (2001) 775.
[72] S.T. Li, G.K. Liu, W. Zhao, Opt. Lett. 24 (1999) 838.
[73] G.K. Liu, S.T. Li, J.V. Beitz, J. Lumin. 83–84 (1999) 343.
[74] M. Kibler, J.C. Gacon, G. Grenet, B. Jacquier, L.C. Brunel, Phys. Stat. Sol. (b) 124 (1984) 731.
[75] Y.R. Shen, W.B. Holzapfel, Phys. Rev. B 51 (1995) 15752.
[76] M. Faucher, D. Garcia, Phys. Rev. B 26 (1982) 5451.
[77] L.S. Gaigerova, O.F. Dudnik, V.F. Zolin, V.A. Kudryashova, in: F. Williams (Ed.), Luminescence of Crystals, Molecules and Solutions, Plenum Press, New York, 1973, p. 514.
[78] Y.K. Voronko, G.V. Maksimova, A.A. Sobol, Opt. Spectrosc. 70 (1991) 203.
[79] X.Y. Chen, W. Zhao, R.E. Cook, G.K. Liu, Phys. Rev. B, in press.
[80] R.P. Leavitt, J. Chem. Phys. 77 (1982) 1661.